

Significant Luminosity Differences of Two Twin Type Ia Supernovae

Ryan J. Foley^{1*}, Samantha L. Hoffmann², Lucas M. Macri³, Adam G. Riess^{4,2}, Peter J. Brown³, Alexei V. Filippenko^{5,6}, Melissa L. Graham⁷, Peter A. Milne⁸

¹*Department of Astronomy and Astrophysics, University of California, Santa Cruz, CA 95064, USA*

²*Space Telescope Science Institute, 3700 San Martin Drive, Baltimore, MD 21218, USA*

³*George P. and Cynthia Woods Mitchell Institute for Fundamental Physics and Astronomy, Department of Physics & Astronomy, Texas A&M University, College Station, TX 77843, USA*

⁴*Department of Physics and Astronomy, Johns Hopkins University, Baltimore, MD, USA*

⁵*Department of Astronomy, University of California, Berkeley, CA 94720-3411, USA*

⁶*Miller Senior Fellow, Miller Institute for Basic Research in Science, University of California, Berkeley, CA 94720, USA*

⁷*Department of Astronomy, University of Washington, Box 351580, U.W., Seattle, WA 98195-1580, USA*

⁸*Steward Observatory, University of Arizona, 933 North Cherry Avenue, Tucson, AZ 85721, USA*

Accepted . Received ; in original form

ABSTRACT

The Type Ia supernovae (SNe Ia) 2011by, hosted in NGC 3972, and 2011fe, hosted in M101, are optical “twins,” having almost identical optical light-curve shapes, colours, and near-maximum-brightness spectra. However, SN 2011fe had significantly more ultraviolet (UV; $1600 < \lambda < 2500 \text{ \AA}$) flux than SN 2011by before and at peak luminosity. Theory suggests that SNe Ia with higher progenitor metallicity should (1) have additional UV opacity near peak and thus lower UV flux; (2) have an essentially unchanged optical spectral-energy distribution; (3) have a similar optical light-curve shape; and (4) because of the excess neutrons, produce more stable Fe-group elements at the expense of radioactive ^{56}Ni and thus have a lower peak luminosity. Foley & Kirshner (2013) suggested that the difference in UV flux between SNe 2011by and 2011fe was the result of their progenitors having significantly different metallicities. The SNe also had a large, but insignificant, difference between their peak absolute magnitudes ($\Delta M_{V, \text{peak}} = 0.60 \pm 0.36 \text{ mag}$), with SN 2011fe being more luminous. We present a new Cepheid-based distance to NGC 3972, significantly improving the precision of the distance measurement for SN 2011by. With these new data, we determine that the SNe have significantly different peak luminosities ($\Delta M_{V, \text{peak}} = 0.335 \pm 0.069 \text{ mag}$), corresponding to SN 2011fe having produced 38% more ^{56}Ni than SN 2011by, and providing additional evidence for progenitor metallicity differences for these SNe. We discuss how progenitor metallicity differences can contribute to the intrinsic scatter for light-curve-shape-corrected SN luminosities, the use of “twin” SNe for measuring distances, and implications for using SNe Ia for constraining cosmological parameters.

Key words: galaxies—individual(M101, NGC 3972), supernovae—general supernovae—individual (SN 2011by, SN 2011fe)

1 INTRODUCTION

Type Ia supernovae (SNe Ia) are excellent standardisable candles that can be measured to cosmological distances. Observations of SNe Ia have been crucial in discovering cosmic acceleration (Riess et al. 1998; Perlmutter et al. 1999), as well as making the most precise measurements of the Hubble constant, H_0 (e.g., Riess et al. 2016), and the equation-of-

state parameter for dark energy, w , (e.g., Jones et al. 2018; Scolnic et al. 2018).

SNe Ia are *not* “standard candles” (just as Cepheid variables are not standard candles, strictly speaking), having a factor of ~ 10 difference in luminosity from one extreme to the other. However, after correcting for light-curve shape (e.g., Phillips 1993) and colour (e.g., Riess et al. 1996; Tripp 1998), SNe Ia have a small scatter in their measured distances (typically $\sim 8\%$; e.g., Hicken et al. 2009; Stritzinger et al. 2011). A corollary to this empirical measurement is

* E-mail:foley@ucsc.edu

that two SNe Ia with exactly the same light-curve shapes, colours, and spectra should have luminosities that differ by at most the intrinsic luminosity scatter that belies additional, unaccounted physical diversity.

One possible driver for the nonzero intrinsic scatter is progenitor stars with differing metallicity. In this case, the number of neutrons increases (alternatively, Y_e decreases) with increasing metallicity. When the star explodes, the additional neutrons result in more stable Fe-group elements at the expense of radioactive ^{56}Ni , which powers the SN light curve and directly affects its peak luminosity (Timmes et al. 2003; Bravo et al. 2010). However, since roughly the same amounts of Fe-group elements are generated, the overall optical opacity is roughly the same, and the light-curve shape and colour are unaffected (Mazzali & Podsiadlowski 2006). Consequently, differing progenitor metallicity could cause the residual luminosity scatter observed among SNe Ia.

In addition to causing larger statistical distance uncertainties, changing progenitor metallicity with redshift could systematically bias the measurement of cosmological parameters (Podsiadlowski et al. 2006). Specifically, if the average progenitor metallicity decreases with increasing redshift, one might expect a drift in the mean peak luminosity of SNe Ia with redshift. Determining if such an effect exists, its magnitude, and its relationship with metallicity is critical for precisely and accurately measuring cosmological parameters with SNe Ia.

While changing progenitor metallicity has a minimal effect on the optical light curves, colours, and spectra of SNe Ia, the ultraviolet (UV) is significantly affected (e.g., Höflich et al. 1998; Lentz et al. 2000; Sauer et al. 2008; Walker et al. 2012). In most models, increasing the progenitor metallicity increases the line blanketing within the outer layers of the ejecta. While these layers quickly become optically thin at longer wavelengths, they remain optically thick to UV photons through peak brightness. As a result, higher metallicity progenitors result in SNe Ia with depressed UV flux relative to the optical flux.

Differences in the UV continuum for low- and high-redshift SNe Ia have been detected in different surveys (Foley et al. 2012a; Maguire et al. 2012; Milne et al. 2015). While these detections are consistent with changing progenitor metallicity with redshift, there could be other effects related to changing populations that do not bias cosmological measurements.

The current sample of low-redshift SNe Ia with high-quality UV spectroscopy is relatively small (Kirshner et al. 1993; Foley et al. 2012b, 2014, 2016; Foley 2013; Foley & Kirshner 2013; Mazzali et al. 2014; Pan et al. 2015). A much larger sample of UV spectra from *Swift* has recently been published (Pan et al. 2018), but the spectra are of lower quality than what is typically obtained with the *Hubble Space Telescope* (*HST*). None the less, the sample of SNe Ia with UV spectra has been critical for understanding the connection between progenitor metallicity, UV properties, and optical luminosity.

In particular, the best indication of different progenitor metallicity for two SNe Ia comes from our studies of SNe 2011by and 2011fe (Foley & Kirshner 2013; Graham et al. 2015; hereafter FK13 and G15, respectively; although see also Milne et al. 2013, Mazzali et al. 2014, and Foley et al. 2016), two “twin” SNe Ia (e.g., Fakhouri et al. 2015) with

nearly identical optical light curves, colours, and spectra, but dramatically different UV colours and spectra. Because of their similar optical properties, the differences in UV behaviour can be constrained to progenitor metallicity (FK13), with the SN 2011by and SN 2011fe progenitors being above and below solar metallicity, respectively. While the SNe have different late-time ($t > 100$ days) optical decline rates, their nebular spectra are nearly identical (G15).

Having established that SNe 2011by and 2011fe likely had substantially different progenitor metallicity, they provide an excellent opportunity to directly determine the effect of metallicity on SN luminosity and distance estimates. Originally, FK13 determined that their peak *V*-band absolute magnitudes differed by ~ 0.6 mag, significantly larger than the intrinsic scatter of SNe Ia. However, this difference directly depends on the distances assumed for these nearby SNe. In particular, while there was a measured Cepheid distance to M101, the host galaxy for SN 2011fe (Shappee & Stanek 2011), there previously was only a Tully-Fisher distance to NGC 3972 (Tully et al. 2009), the host galaxy of SN 2011by. The latter had a relatively large uncertainty (0.36 mag), and systematic differences between the Cepheid and Tully-Fisher scale could have been the main cause for the apparently large differences in SN luminosity.

To reduce this source of uncertainty, we obtained a series of *HST* images to find Cepheid variable stars in NGC 3972 and measure both a precise absolute distance to NGC 3972 and a relative distance between M101 and NGC 3972, removing uncertainties common to both measurements. From this analysis, we find that the distance to NGC 3972 is similar to the Tully-Fisher measurement (although with a shift of 0.26 mag), and SNe 2011by and 2011fe do indeed have significantly different luminosities.

We present our *HST* observations in Section 2. We detail our Cepheid distance estimates, direct luminosity comparisons of the SNe, and direct SN distance estimates in Section 3. We discuss the implications of this result and conclude in Section 4.

2 OBSERVATIONS

2.1 Cepheids in NGC 3972

To obtain a precise Cepheid distance to NGC 3972, we observed the galaxy using the *HST* Wide-Field Camera 3 (WFC3) UVIS and infrared (IR) channels (Programme GO-13647; PI Foley). Details of the UVIS and IR observations and data reduction are presented by Hoffmann et al. (2016) and Riess et al. (2016), respectively. Here we briefly review them.

Observations with WFC3/UVIS and the F350LP “white light” filter were used to discover Cepheids and measure their periods. The data were obtained over 12 separate epochs, with the specific timing chosen to minimise the integral of the power over the frequency interval corresponding to the observation window. For 6 epochs, we also obtained observations with WFC3/IR and the F160W (roughly *H*) filter. For the other 6 epochs, half had an observation with WFC3/UVIS and the F555W (roughly *V*) filter and the other half had an observation with WFC3/UVIS and the F814W (“wide *I*”) filter. The filtered observations are used primarily to aid in selection and to constrain dust reddening.

Table 1. *HST*/STIS Spectral Observations of SN 2011by

Phase ^a	UT Date	Exposure (s) ^b
−9.1	2011 Apr. 30.522	8300+2263 ^c
−4.7	2011 May 5.139	0+2263
−0.4	2011 May 9.343	5316+2263 ^d
3.0	2011 May 13.749	0+2263
8.8	2011 May 18.203	0+2263

^aDays since *B* maximum, 2014 Feb. 2.0 (JD 2,456,690.5).

^bFirst and second numbers correspond to the time for the G230L and G430L gratings, respectively.

^cOriginally published by G15.

^dG430L data originally published by Maguire et al. (2012); G230L data originally published by FK13.

The first and last epochs were obtained on 19 April 2015 and 8 July 2015 UT, respectively, corresponding to an 80-day baseline. Data were retrieved from the Mikulski Archive for Space Telescopes (MAST) and reduced as described by Hoffmann et al. (2016) and Riess et al. (2016). An *HST*/WFC3 image of NGC 3972 is shown in Figure 1.

Photometry was performed with DAOPHOT/ALLSTAR (Stetson 1987) and ALLFRAME (Stetson 1994) using point-spread functions (PSFs) created with TinyTim (Krist et al. 2011) as described by Macri et al. (2006), Riess et al. (2009), Riess et al. (2011), and Hoffmann et al. (2016).

2.2 *HST* Spectra of SN 2011by

Optical spectra of SN 2011by were obtained with *HST*/STIS (Programme GO–12298; PI Ellis). STIS produces excellent absolute and relative spectrophotometry, and therefore the relative luminosity as a function of wavelength for similar-phase spectra can be used to determine the relative reddening of two twin SNe.

SN 2011by was observed with STIS on 5 epochs, although only two use a UV setting. The two UV/optical spectra were presented by Maguire et al. (2012, but only the optical portion), FK13, and G15. The remaining spectra are first presented here. The data were reduced using the standard *HST* Space Telescope Science Data Analysis System (STSDAS) routines to bias-subtract, flat-field, extract, wavelength-calibrate, and flux-calibrate each SN spectrum. Similar reductions were performed for the SN 2011fe spectra used in this study (Foley et al. 2012b, 2014, 2016; Foley & Kirshner 2013; Foley 2013; Pan et al. 2015). A log of all observations is presented in Table 1. The SN 2011by spectra are shown in Figure 2.

3 ANALYSIS

3.1 Selecting Cepheids in NGC 3972

First, the F350LP light curves of all sources were examined to determine the subset that are variable. We visually

inspected the light curves and rejected obviously spurious photometry and photometry with unusually large uncertainties. The Welch-Stetson variability index (Stetson 1996) was used to determine which objects are variable.

We matched the light curves of all sources with template Cepheid light curves (Yoachim et al. 2009) of periods between 10 and 100 days. All data (regardless of band) were used for the fitting. From the best-fitting period, the model predicts a corresponding amplitude. Comparing the predicted amplitude to the F350LP light curve, we measured the χ^2 statistic. More than 90% of the objects selected as variable were poorly matched by the Cepheid template light curves. For the remaining subset, we further refined the best-fitting parameters. Finally, we used additional criteria to remove objects that are inconsistent with isolated low-to-moderate-reddening Cepheids.

In total, we selected 71 Cepheids. We present a finding chart of NGC 3972 with the Cepheids marked in Figure 1. Details of the selection process can be found in Hoffmann et al. (2016).

3.2 Cepheid Distance for NGC 3972

As was done by Riess et al. (2016), we use the period-luminosity relation (Figure 3), correcting for metallicity, and a combination of NGC 4258, the Milky Way, and the Large Magellanic Cloud (LMC) as an anchor to determine the distance of NGC 3972. We refer the reader to Riess et al. (2016) for details of this calculation.

For all measured Cepheids, we determine the Wesenheit magnitude (Madore 1982), which corrects for extinction and the finite temperature width of the instability strip. We compute a period-luminosity relation and remove significant outliers as well as Cepheids with periods below the completeness limit (see Riess et al. 2016). Figure 3 displays the final period-luminosity relation for NGC 3972, consisting of 42 Cepheids. The Cepheid data imply a distance modulus of 31.594 ± 0.071 mag.

Additionally, we can directly compare the Cepheid data for NGC 3972 and M101 to determine their relative distances without the uncertainties of the absolute distance scale. The relative distance is particularly important for comparing SNe 2011by and 2011fe. Directly comparing the Cepheid data for both galaxies and accounting for covariances in the measurements, we determine that NGC 3972 has a distance modulus that is 2.459 ± 0.062 mag greater than that of M101¹.

3.3 Luminosity Differences for SNe 2011by and 2011fe

With the absolute and relative distances to M101 and NGC 3972, we can directly compare the observations of SNe 2011by and 2011fe on an absolute scale. However, to

¹ We use the Riess et al. (2016) determination of the Cepheid distance for M101 ($\mu = 29.14$ mag) rather than that of Shappee & Stanek (2011, $\mu = 29.04$ mag). Primarily, this is so that both galaxies have consistent methodology. However, we note that the measurements are consistent (to within 0.01 mag) when the same LMC or NGC 4258 zeropoints are used.

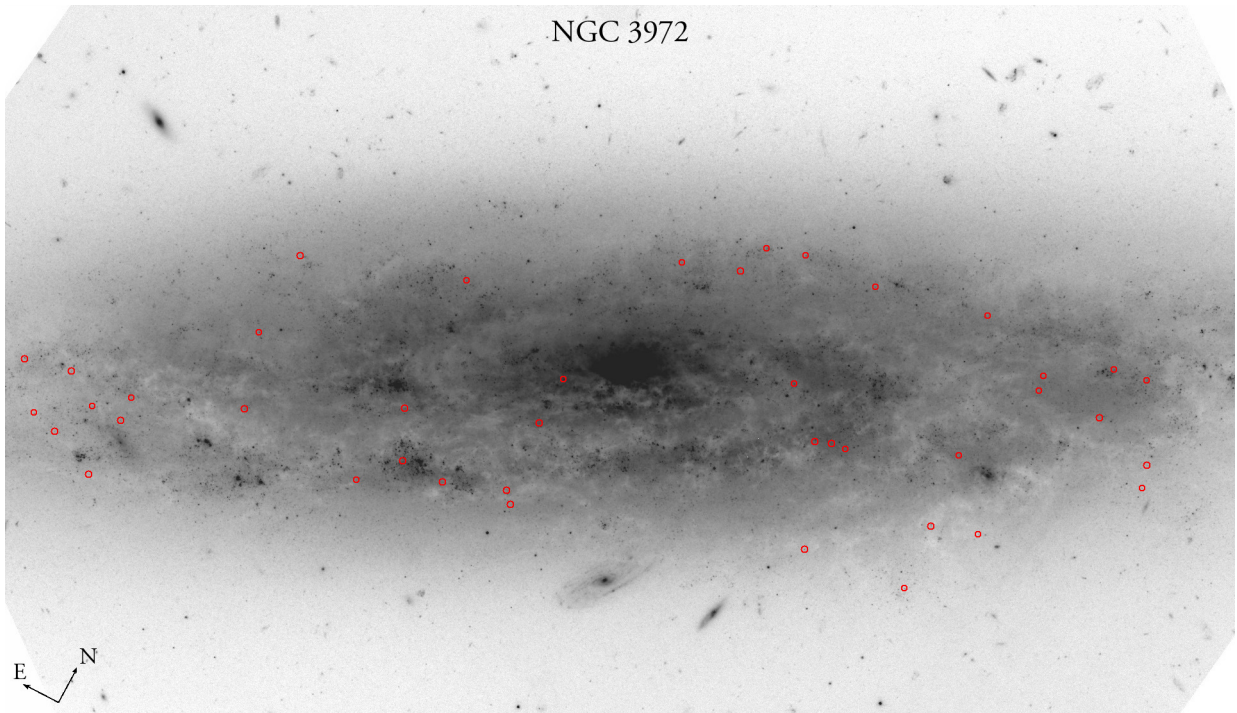


Figure 1. $90'' \times 160''$ *HST*/WFC3 F350LP image of NGC 3972. The image is generated from the stack of all F350LP data and the intensity scale is logarithmic. To aid orientation, a compass rose is shown, with each arrow corresponding to $5''$. The positions of Cepheid variables used to determine the distance to NGC 3972 are marked with red circles.

do this, one must correct for any host-galaxy extinction. While both SNe are consistent with having zero reddening, SN 2011by is slightly redder than SN 2011fe. In order to account for the possibility of a different reddening for each SN and a coherent, grey offset in their absolute magnitudes, we simultaneously fit for both.

Conveniently, SNe 2011by and 2011fe were both observed by *Swift* (Brown et al. 2012; Milne et al. 2013) and the Lick Observatory 0.76 m Katzman Automatic Imaging Telescope (KAIT; Silverman et al. 2013; Zhang et al. 2016), making *S*-corrections (Stritzinger et al. 2002) unnecessary (and thus removing one potential systematic uncertainty). Unfortunately, near peak brightness, SN 2011fe was too bright to have accurate flux measurements in the *Swift* *UBV* bands. As a result, there is a small phase range of only a few days, far from peak, where both SNe have *Swift* *B* photometry; it is therefore difficult to determine a precise offset in this band and these data are not used in our analysis. Because of potential intrinsic UV differences among the two SNe, we also do not use the *U*-band (and bluer bands) *Swift* data to measure the reddening. However, both SNe have sufficient overlap in *Swift* *V* to determine a magnitude offset in that band.

Additionally, Matheson et al. (2012) observed SN 2011fe in *JH* and Friedman et al. (2015) observed SN 2011by in *JHK_s*. While each SN was observed with different telescopes, instruments, and slightly different filters, we were able to determine the necessary *S*-corrections using the SN 2011fe near-infrared (NIR) spectral sequence (Hsiao et al. 2013)

and the available filter functions² (Cohen et al. 2003). This process is similar to what was done by Weyant et al. (2018) for comparing SNe Ia in these two systems.

Using their peak-brightness spectra, we measured a *K*-correction for each SN. The relative *K*-correction was <0.012 mag for all bands.

Correcting for Milky Way extinction (Schlafly & Finkbeiner 2011), *K*-corrections, *S*-corrections (for *JH*), and their distances, we produce absolute magnitude light curves in *BVR_IJH*, which we present in Figure 4. We note that the absolute magnitude light curves are not corrected for any potential host-galaxy extinction. To determine the relative magnitude offset in each band, we use a b-spline function to interpolate each light curve to match the phases for the other light curve. We then fit for an offset between the two light curves. These offsets, as a function of effective filter wavelength (as determined from the peak-brightness SN 2011fe spectrum), are presented in Figure 5. In all bands, SN 2011fe is 0.31 to 0.48 mag more luminous than SN 2011by, with bluer bands having a larger offset. As a cross-check, Dhawan et al. (2018) found a difference in the peak absolute *J* magnitude of 0.30 mag, comparable to our full light-curve *J*-band offset of 0.32 mag, using the same data. The average offset in all bands is 0.411 ± 0.007 mag, but a single offset for all bands does not fit the data well, having $\chi^2/\text{dof} = 80.1/6$.

Notably, the offset between SNe 2011by and 2011fe in a given band is similar at all epochs probed by the photometry. The one exception is for the *J* band for phases between ~ 10

² <https://www.noao.edu/kpno/manuals/whirc/filters.html>

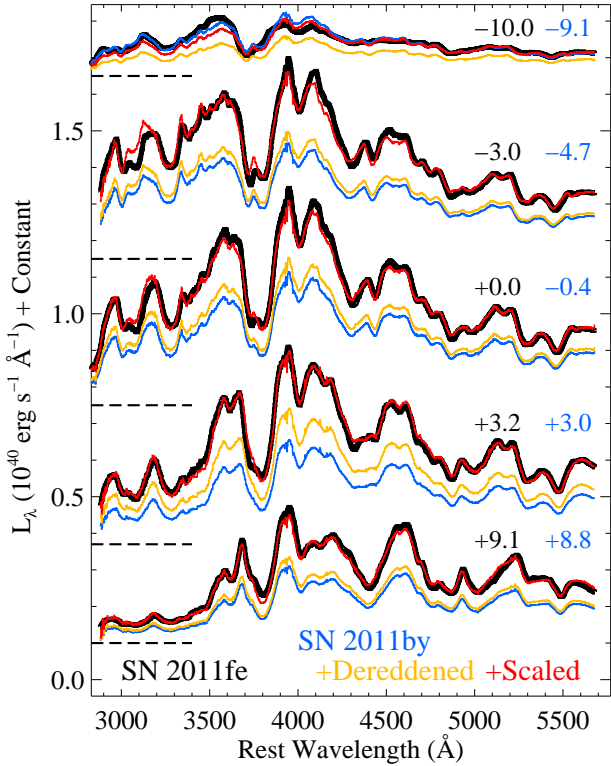


Figure 2. *HST*/STIS spectra of SNe 2011by (blue curves) and 2011fe (black curves) for 5 matched phases with each phase labeled next to the spectra. The spectra have been scaled by their geometric dilution factor so that they are in L_λ units. The spectra have been shifted vertically by arbitrary amounts indicated by the dashed lines. Also plotted are the SN 2011by spectra after being dereddened (gold curves) and scaled (red curves) to match the corresponding SN 2011fe spectra using the best-fitting values for both $E(B - V)$ and the scale factor, as discussed in the text. For all but the first epoch, the similarity in spectral shape and features is striking.

and ~ 25 days after peak brightness. This indicates that the intrinsic colour evolution for the SNe is similar and that the offsets in a given band are primarily caused by slow-changing attributes such as a luminosity offset and dust extinction.

Assuming that the change in absolute magnitude offset with wavelength is caused by differential dust reddening, we simultaneously fit for a constant offset and dust reddening. Using either a [Cardelli et al. \(1989\)](#) or [Fitzpatrick \(1999\)](#) reddening law, and fixing R_V to be 3.1, we find consistent reddening values with $E(B - V) \approx 0.047$ mag. If we allow R_V to float, then we find best-fit values for $E(B - V)$ of ~ 0.038 mag with $R_V \approx 4.2$. Regardless of the choice of reddening law, the constant offset is ~ 0.27 mag. For our final analysis, we use the [Fitzpatrick \(1999\)](#) reddening law.

To further constrain the reddening, we examine the spectrophotometry of SNe 2011by and 2011fe. Optical spectra of both SNe were obtained with *HST*/STIS. SN 2011fe was observed on 10 separate epochs covering phases of -13 to $+40$ days ([Maguire et al. 2012](#); [Foley 2013](#); [Foley & Kirshner 2013](#); [Mazzali et al. 2014](#)).

We match each SN 2011by spectrum to a SN 2011fe spectrum with a similar phase (to within ~ 1 day). Specifically, the -9.1 , -4.7 , -0.4 , 3.0 , and 8.8 -day SN 2011by

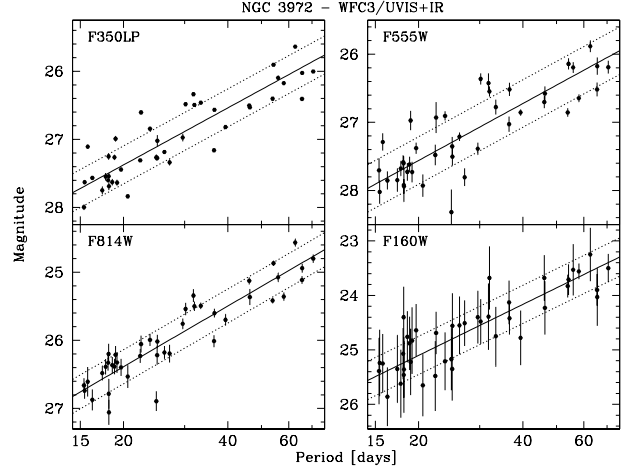


Figure 3. Period-luminosity relations (Leavitt laws) for the Cepheid variables in NGC 3972 in the *HST*/WFC3 F350LP (upper left), F555W (upper right), F814W (lower left), and F160W (lower right) filters.

spectra are matched to -10.0 , -3.0 , 0.0 , 3.2 , and 9.1 -day SN 2011fe spectra, respectively. With a small phase difference between spectra, spectral feature differences should be minimal, especially for such similar SNe. After correcting for Milky Way reddening and their distances, each SN 2011by spectrum is dereddened (to account for potential host-galaxy reddening) and scaled to match its corresponding Milky Way-dereddened SN 2011fe spectrum. Since the phases are not perfectly matched, we do not expect the flux scaling, which corresponds to an achromatic offset, to be correct; however, the colour evolution between these epochs should generally be small, allowing for an accurate measurement of the reddening. This method is graphically outlined in [Figure 2](#).

Using a [Fitzpatrick \(1999\)](#) reddening law with $R_V = 3.1$, we find that the reddening of SN 2011by (relative to SN 2011fe) ranges from $E(B - V) = -0.11$ mag (i.e., SN 2011by is redder) to 0.06 mag, with 3/5 of the epochs having $E(B - V) = 0.023$ to 0.027 mag. Only the first epoch has “negative reddening,” which we consider to be the result of a combination of a quickly changing spectral energy distribution (SED) at these early times and a phase difference of 0.9 day. Ignoring the first epoch, the remaining epochs have an average reddening of $E(B - V) = 0.039 \pm 0.006$ mag, which we consider to be our best estimate of the host-galaxy reddening of SN 2011by relative to that of SN 2011fe. Fixing the reddening to this value, the best-fitting coherent absolute magnitude offset is 0.303 ± 0.006 mag. We note that the uncertainty on this number neglects the distance uncertainty and reddening uncertainty (as the reddening was fixed).

Assuming no host-galaxy dust reddening for SN 2011fe and $E(B - V) = 0.039 \pm 0.006$ mag for SN 2011by, the peak V -band absolute magnitude for each SN is -19.18 ± 0.05 mag and -18.85 ± 0.07 mag, respectively. The majority of the uncertainties in these values is related to the distances, as determined from the Cepheid measurements. Since the distance estimates are obtained through the same method, several sources of uncertainty do not apply to a relative distance

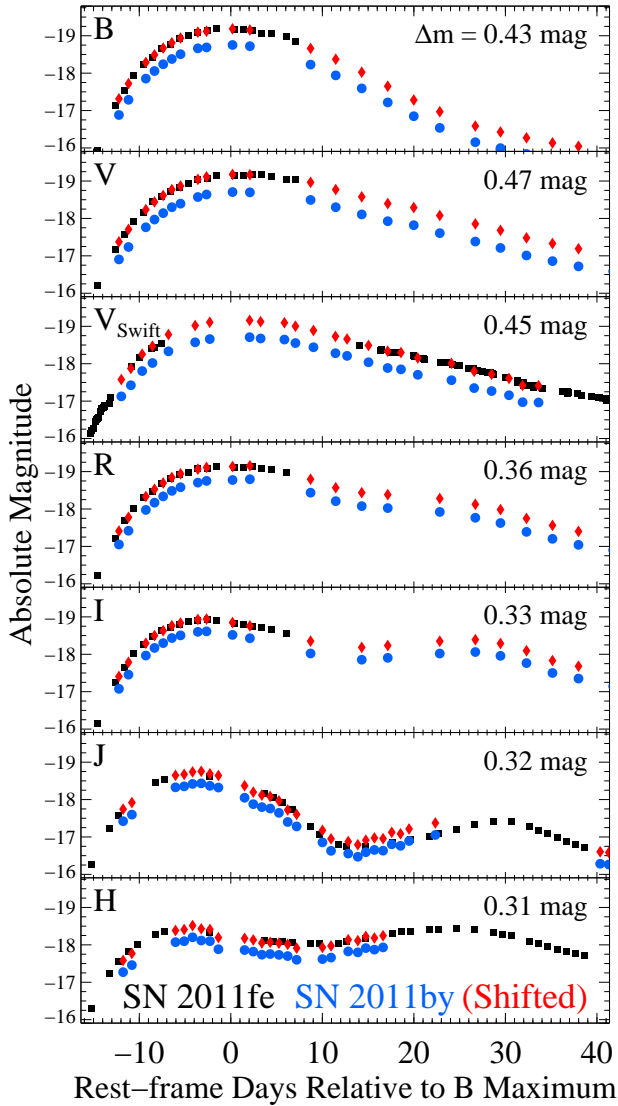


Figure 4. Optical and NIR light curves of SNe 2011by (blue circles) and 2011fe (black squares) in KAIT *BVRI*, *Swift V*, and *JH* bands. The red diamonds represent the SN 2011by light curve shifted by a single magnitude for each band, noted in each sub-panel, to match the luminosity of SN 2011fe.

measurement. Taking our best estimates for different terms, we can determine the relative peak *V*-band absolute magnitude and uncertainty,

$$\Delta M_V = \Delta m - \Delta E(B - V)R_V - \Delta\mu, \quad (1)$$

$$\sigma_{\Delta M_V} = \left(\sigma_{\Delta m}^2 + (3.1\sigma_{E(B-V)})^2 + \sigma_{\Delta\mu}^2 \right)^{1/2}, \quad (2)$$

with parameters and uncertainties

$$(\Delta m, \Delta E(B - V), R_V, \Delta\mu) = (2.93, 0.044, 3.1, 2.449), \quad (3)$$

$$(\sigma_{\Delta m}, \sigma_{E(B-V)}, \sigma_{\Delta\mu}) = (0.007, 0.006, 0.062), \quad (4)$$

where $\Delta E(B - V)$ is the total difference in reddening, including the Milky Way contribution. We therefore find

$$\Delta M_V = 0.335 \pm 0.063 \text{ mag}, \quad (5)$$

with SN 2011fe being more luminous. The difference is

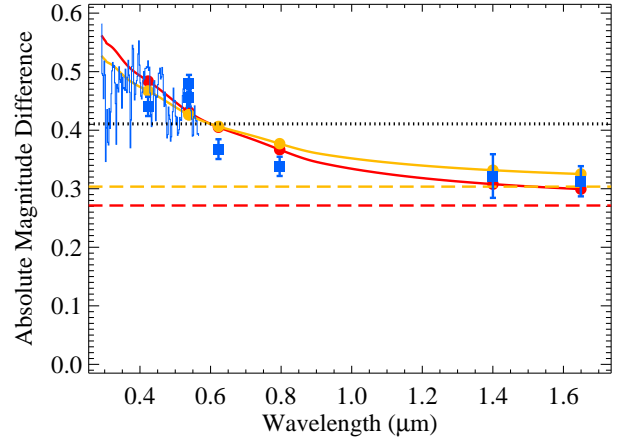


Figure 5. Absolute magnitude difference between SNe 2011by and 2011fe as a function of wavelength. The blue squares show the KAIT *BVRI*, *Swift V*, and *JH* bands. The effective wavelength for each point is determined by convolving the filter transmission functions with the peak-brightness spectrum. The blue curve represents the difference in their peak-brightness *HST/STIS* spectra. The black dotted line illustrates the best-fitting constant offset to all data. The red and gold solid lines represent the best-fitting reddening and offset model (using a [Fitzpatrick 1999](#) reddening law with $R_V = 3.1$) when only fitting the photometry and varying the reddening and the photometry to determine the offset, respectively. The red and gold dashed lines display the corresponding constant offsets. Our best-estimate reddening is $E(B - V) = 0.039 \pm 0.006$ mag and best-estimate constant offset is 0.304 ± 0.062 mag, which corresponds to the gold dashed line.

consistent with, but smaller than, that found by [FK13](#): 0.60 ± 0.36 mag. It is also consistent with the [Riess et al. \(2016\)](#) difference (0.286 mag), which only used optical light-curve data. If one also makes a 0.06 mag host-mass correction (e.g., [Kelly et al. 2010](#); [Lampeitl et al. 2010](#); [Sullivan et al. 2010](#), see Section 4), there is no difference between our measurement and that of [Riess et al. \(2016\)](#). With the updated relative distances, we find that SNe 2011by and 2011fe had peak *V*-band absolute magnitudes which were significantly different, with a significance of 4.9σ . Furthermore, we find a coherent, reddening-free (Wesenheit) offset of 0.314 ± 0.062 mag, corresponding to a significance of 5.1σ .

We present updated absolute *V*-band light curves in Figure 6 to illustrate these differences. This figure uses an expanded set of light-curve data from a variety of sources (see [G15](#), and references therein) to show the full evolution of SNe 2011by and 2011fe for ~ 1 yr after explosion.

The grey magnitude offset corresponds to a difference in peak bolometric luminosity. SNe 2011by and 2011fe have practically indistinguishable maximum-light (as well as essentially all other epochs) optical spectra ([FK13](#); [G15](#)), light-curve shapes ([FK13](#)), and colour curves ([G15](#)). Therefore, their bolometric corrections must be similar. While their UV spectra are different, this will have a minor effect on the bolometric luminosity (at most a few percent); it is also in the direction of SN 2011fe having a higher bolometric luminosity than of SN 2011by, which would make their luminosities even more discrepant. While it is possible that their mid-IR and far-IR emission is significantly different,

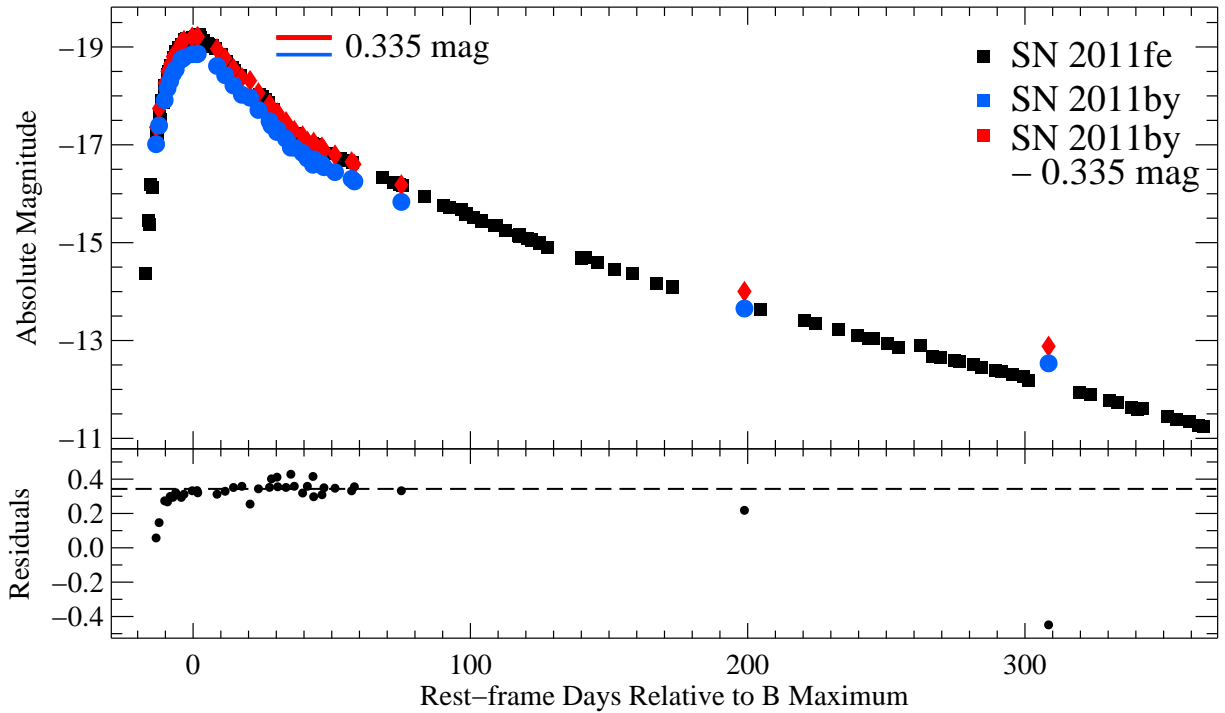


Figure 6. *Top:* Absolute V -band light curves of SNe 2011by (blue circles) and 2011fe (black squares) as presented by G15, but adjusted to account for the new distances to each SN and the measured host-galaxy extinction for SN 2011by. The SN 2011fe light curve is a combination of data from Richmond & Smith (2012), G15, and Zhang et al. (2016). The SN 2011by data are from Silverman et al. (2013) and G15. Also plotted is the SN 2011by light curve shifted by 0.335 mag, corresponding to the difference in peak brightness between the two SNe. *Bottom:* Difference between the absolute V -band light curves for SN 2011by and SN 2011fe, where the SN 2011fe light curve was interpolated to match the epochs of the SN 2011by observations. The dashed line is at 0.335 mag.

this is unlikely given all other evidence, and should have a small overall effect on the bolometric luminosity.

To determine the peak bolometric luminosity, we use the peak spectra for the two SNe (FK13), which cover the rest-frame wavelengths $\sim 1600 - 10,200 \text{ \AA}$ for both SNe. We then extend the spectra to the NIR by extrapolating an 18,000 K blackbody whose flux is matched to the optical data. Since we mostly care about the relative luminosities, the exact NIR SED is not especially important. Integrating the spectra and using the distance measurements for each SN, we find peak bolometric luminosities of $(9.3 \pm 0.7) \times 10^{42}$ and $(12.9 \pm 0.7) \times 10^{42} \text{ erg s}^{-1}$ for SNe 2011by and 2011fe, respectively.

To determine the ^{56}Ni mass, we use the common formula,

$$M_{^{56}\text{Ni}} = \frac{L_{\text{bol, max}}}{\alpha \dot{S}(t_{r, \text{bol}})}, \quad (6)$$

where α is a unitless parameter of order unity that describes the diffusion of radiation through the ejecta, \dot{S} is the instantaneous rate of energy injection from radioactive decay, and $t_{r, \text{bol}}$ is the bolometric rise time (see e.g., Arnett 1982; Jeffery 1999). For this analysis, we use $\alpha = 1 \pm 0.2$, which is a common choice (e.g., Stritzinger et al. 2006). Others have chosen a slightly higher value for α ($\alpha = 1.2 \pm 0.2$; Scalzo et al. 2010; Pereira et al. 2013); however, the exact choice does not affect our main result, which examines the ratio of ^{56}Ni masses.

For this analysis, we use a bolometric rise time of

$t_{r, \text{bol}} = 16.58 \pm 0.14$ days for SN 2011fe (Pereira et al. 2013), and assume that SN 2011by has the same rise time. This assumption is reasonable given the similar light-curve shapes and colour curves for the two SNe. We note that there is some evidence of SN 2011by having a slightly slower V -band rise (Figure 6); however, G15 found that the SN 2011fe rise time was 0.6 ± 0.4 days longer than that of SN 2011by (opposite of what one might immediately assume from the differences in the V band). Changing the rise time by a day in either direction only affects the SN 2011by ^{56}Ni mass by $0.02 M_{\odot}$. Using Equation 6, we find ^{56}Ni masses of 0.43 ± 0.09 and $0.59 \pm 0.12 M_{\odot}$ for SNe 2011by and 2011fe, respectively, where the largest component of the uncertainty is from α .

For the above calculation, we propagated the uncertainty from several different sources (rise time, α , etc) that are likely the same for both SNe. In the scenario where these values are the same for both SNe, but the exact value is uncertain, we can measure the ratio of the ^{56}Ni masses with an uncertainty which does not include the uncertainties of these different values. Doing this, we find a ^{56}Ni ratio of $M_{11\text{fe}}(^{56}\text{Ni})/M_{11\text{by}}(^{56}\text{Ni}) = 1.38 \pm 0.09$. This value is similar to that found by FK13 (1.7), but slightly lower, which is unsurprising given the similar, but slightly different luminosities for the two analyses. With the assumptions listed above, the two SNe have significantly different ^{56}Ni masses, with 4.2σ significance.

Table 2. Supernova and Host-Galaxy Properties

Parameter	SN 2011by	SN 2011fe
Galaxy	NGC 3972	M101
μ (mag)	31.594 (0.071)	29.135 (0.047)
V_{peak} (mag)	12.91 (0.01) ^F	9.98 (0.02) ^P
$\Delta m_{15}(B)$ (mag)	1.14 (0.03) ^S	1.10 (0.04) ^P
$E(B - V)_{\text{MW}}$ (mag)	0.013	0.008
$E(B - V)_{\text{host}}$ (mag)	0.039 (0.006)	0
$M_{V, \text{peak}}$ (mag)	-18.85 (0.07)	-19.18 (0.05)
Peak Bol. Lum. (10^{42} erg s ⁻¹)	9.3 (0.7)	12.9 (0.7)
⁵⁶ Ni Mass (M_{\odot})	0.43 (0.09)	0.59 (0.12)
$M_{V, \text{peak}}$ Offset (mag)	0.33 (0.07)	0
⁵⁶ Ni Mass Ratio (Rel. to 11by)	1	1.38 (0.09)
P99 $M_{V, \text{peak}}$ Offset (mag)	0.028 (0.022)	0
SALT μ (mag)	31.96 (0.04)	29.16 (0.06)
SALT M_B Offset (mag)	0.16 (0.08)	0
Cepheid-SN μ Offset (mag)	-0.14 (0.08)	+0.15 (0.08)

Note. — F = FK13; P = [Pereira et al. \(2013\)](#); S = [Silverman et al. \(2013\)](#).

3.4 Light-curve Distance Estimates

In the previous section, we determined that SNe 2011by and 2011fe had significantly different luminosities and ⁵⁶Ni masses. However, these SNe do not fall outside the range of all SNe Ia. For measuring distances with SNe Ia, differences in light-curve shape and colour make SNe with different intrinsic luminosities have similar *corrected luminosities*. SNe 2011by and 2011fe have very similar observational properties, and thus it would be unlikely for these twin SNe to have the significantly different corrected luminosities.

None the less, we go through this exercise below. Importantly, we must consider the intrinsic scatter for a given distance-fitting algorithm to determine the significance of any difference. The intrinsic scatter indicates how much diversity in distances there is after correcting for photometric parameters and can be the result of additional physical conditions such as metallicity. If SNe 2011by and 2011fe are different by less than the intrinsic scatter, they would not represent outliers for measuring cosmological parameters. However, whatever causes the differences in their peak luminosity would likely contribute to the overall intrinsic scatter measured for large samples of objects.

The simplest approach to determine the expected difference in $M_{V, \text{peak}}$ is to use the decline-rate parameter, $\Delta m_{15}(B)$. [Phillips et al. \(1999\)](#) determined empirical equations for this relation that are independent of colour. For the V band, they find

$$\Delta M_{V, \text{peak}} = 0.672(\Delta m_{15}(B) - 1.1) + 0.633(\Delta m_{15}(B) - 1.1)^2, \quad (7)$$

where the difference is explicitly relative to a SN with $\Delta m_{15}(B) = 1.1$ mag. Since SN 2011fe conveniently has exactly this value, the equation can be used to determine the expected difference between SNe 2011by and 2011fe, yielding 0.028 ± 0.022 mag, with SN 2011fe expected to be slightly (insignificantly) more luminous. As expected, based on the light-curve shape alone, the two SNe are expected to have nearly identical peak luminosities.

One can now test how different the relative distances derived from the light-curve shape and apparent brightness

of SNe 2011by and 2011fe are from those directly measured from Cepheids. The difference between these two methods reduces to a difference in peak absolute magnitudes, as determined by both methods. This difference is 0.44 ± 0.11 mag, including an intrinsic scatter term of 0.09 mag (as determined by [Phillips et al. 1999](#)) for the uncertainty. This difference is 3.8σ significant.

We also used the SALT2 algorithm ([Guy et al. 2007](#)) to determine the distances and peak absolute magnitudes of the two SNe. SALT2 simultaneously fits multiple light curves, which should include subtle differences in colour and light-curve shape in any distance estimate.

The difference between SALT2-estimated B -band absolute magnitudes is 0.16 ± 0.08 mag, consistent with that found with the [Phillips et al. \(1999\)](#) method, and consistent with zero offset in absolute magnitude. Since the SALT2 method corrects for colour differences, which could be caused by reddening, this value should be compared to the difference in A_B estimated from a direct comparison of the SN light curves,

$$A_B = R_B \times E(B - V) = 4.1 \times (0.039 \pm 0.006) \text{ mag} \quad (8) \\ = 0.160 \pm 0.025 \text{ mag.}$$

Therefore, SALT2 is measuring the slight colour difference between the two SNe, but is incapable of measuring the grey offset between them. In other words, SALT2 expects SNe 2011by and 2011fe to have the same intrinsic luminosities. As a result, the difference in Hubble residuals (HRs) for the two SNe is approximately the difference between the reddening-uncorrected ΔM_V and the SALT2 difference: $\Delta \text{HR} = 0.33$ mag. This is similar to what was seen by [Riess et al. \(2016\)](#), finding $\Delta \text{HR} = 0.29$ mag using SALT2.

[Riess et al. \(2016\)](#) found that SNe 2011by and 2011fe have HRs of -0.14 and 0.15 mag, respectively, making neither an outlier relative to the scatter. On the other hand, it is perhaps a coincidence that SN 2011by is faint relative to the mean of the sample and SN 2011fe is bright relative to the mean of the sample. If either SN 2011by (SN 2011fe) were replaced with a true copy of SN 2011fe (SN 2011by), the mean absolute magnitude of the 19 Cepheid-SN calibrators would shift by -0.016 mag ($+0.019$ mag). This shifts the value of H_0 by 0.72% to 0.86%, changing the best-estimate [Riess et al. \(2016\)](#) value of H_0 of 73.24 km s⁻¹ Mpc⁻¹ to 72.71 and 73.87 km s⁻¹ Mpc⁻¹, respectively. This would be a small change to the value of H_0 ; however, the relatively small size of the Cepheid-SN calibrator sample, where individual objects can influence the measured value of H_0 , will clearly be a limiting factor in the very near future.

4 DISCUSSION AND CONCLUSIONS

We find that SNe 2011by and 2011fe, despite having nearly identical optical spectral sequences ([G15](#)) and light-curve shapes/colours ([FK13](#); [G15](#)), have different peak luminosities. This result is similar to that of [FK13](#) — but with our new Cepheid distance to NGC 3972, this result is highly statistically significant. The observations suggest that SN 2011fe generated 38% more ⁵⁶Ni than SN 2011by. Furthermore, the differences in luminosity are significantly larger than the intrinsic luminosity scatter for SNe Ia.

The one substantial luminosity-independent observational difference between SNe 2011by and 2011fe is their near-peak UV flux difference (FK13; G15). SN 2011fe had relatively more UV flux and a higher peak bolometric luminosity than SN 2011by, both of which were predictions for a SN with relatively low progenitor metallicity (Timmes et al. 2003; Mazzali & Podsiadlowski 2006). Our current observations are further indication that the progenitors of SNe 2011by and 2011fe had super-solar and sub-solar metallicity, respectively (FK13; Mazzali et al. 2014; G15).

If SNe Ia were perfectly described by their optical light-curve shape and colour, then SNe 2011by and 2011fe should have the same peak luminosity. The difference in luminosities indicates that additional unaccounted physics must increase the scatter of SN Ia measurements beyond errors in analysis. This comparison indicates that progenitor metallicity is likely a large component of the “intrinsic scatter.” However, current distance estimators do not consider SNe 2011by and 2011fe significantly different (in part because of their internal model uncertainties and in part because of the intrinsic scatter), and thus neither would necessarily be excluded from a cosmological analysis. Their inclusion as SN-Cepheid calibrators has a minimal impact on the value of H_0 , but will be limiting in the near future if the size of the calibrator sample is not increased significantly.

Recent cosmological analyses have found a significant offset in the average Hubble residual between SNe Ia in low-mass and high-mass galaxies (Kelly et al. 2010; Lampeitl et al. 2010; Sullivan et al. 2010). Although the exact functional form of any relation is not known (e.g., Childress et al. 2013), a correction is often applied as a step function in host-galaxy stellar masses with the step at $10^{10} M_{\odot}$. While this effect has not been significant in all analyses (e.g., Scolnic et al. 2018), a typical value for the difference is ~ 0.06 mag, with SNe Ia in low-mass galaxies being fainter. Our results are broadly consistent with this trend, where NGC 3972 and M101 have stellar masses below and above $10^{10} M_{\odot}$, respectively. It is therefore possible that the mass step is driven primarily by metallicity differences in the progenitor systems which correlate with the host galaxy’s total stellar mass at the time of explosion.

A recent analysis of “twin” SNe Ia suggested a low intrinsic dispersion of only 0.08 mag (Fakhouri et al. 2015). SNe 2011by and 2011fe are, by all accounts, better twins than those presented by Fakhouri et al. (2015), yet they have a peak absolute magnitude difference that is ~ 4 times larger than the scatter for their sample. While choosing SNe Ia with similar spectral properties should not typically increase scatter, the incredibly well-observed and precisely measured SNe 2011by and 2011fe provide a cautionary tale for using this method for improving distance estimates.

Future analyses must evaluate how this result will affect their conclusions. Obviously, there is additional information in the UV SED, and observing the rest-frame UV could potentially improve SN Ia distance estimates. However, if the average progenitor metallicity is changing with redshift (e.g., Childress et al. 2014), there may be a systematic bias to SN Ia distances with redshift. As there is some indication of changing UV properties with redshift (Foley et al. 2012a; Maguire et al. 2012; Milne et al. 2015), a thorough analysis of this effect should be performed. In particular, additional UV spectra of low-redshift SNe Ia will be critical for under-

standing how progenitor metallicity affects SN Ia distance estimates.

ACKNOWLEDGEMENTS

Facility: HST (ACS, STIS, WFC3)

Based on observations made with the NASA/ESA *Hubble Space Telescope*, obtained at the Space Telescope Science Institute (STScI), which is operated by the Association of Universities for Research in Astronomy, Inc., under National Aeronautics and Space Administration (NASA) contract NAS 5–26555. These observations are associated with Programmes GO–12298 and GO–13647. Support for GO–13647 was provided by NASA through a grant from STScI. This manuscript is based upon work supported by NASA under Contract No. NNG16PJ34C issued through the *WFIRST* Science Investigation Teams Programme.

The UCSC team is supported in part by NASA grant NNG17PX03C, NSF grant AST-1518052, the Gordon & Betty Moore Foundation, the Heising-Simons Foundation, and by fellowships from the Alfred P. Sloan Foundation and the David and Lucile Packard Foundation to R.J.F.

P.J.B./the *Swift* Optical/Ultraviolet Supernova Archive (SOUSA) and P.A.M. are supported by NASA’s Astrophysics Data Analysis Program through grants NNX13AF35G and NNX17AF15G, respectively. A.V.F. is grateful for assistance from the Christopher R. Redlich Fund, the TABASGO Foundation, and the Miller Institute for Basic Research in Science (U.C. Berkeley). KAIT and its ongoing operation were made possible by donations from Sun Microsystems, Inc., the Hewlett-Packard Company, AutoScope Corporation, Lick Observatory, the NSF, the University of California, the Sylvia & Jim Katzman Foundation, and the TABASGO Foundation.

REFERENCES

- Arnett W. D., 1982, *ApJ*, **253**, 785
 Bravo E., Domínguez I., Badenes C., Piersanti L., Straniero O., 2010, *ApJ*, **711**, L66
 Brown P. J., et al., 2012, *ApJ*, **753**, 22
 Cardelli J. A., Clayton G. C., Mathis J. S., 1989, *ApJ*, **345**, 245
 Childress M., et al., 2013, *ApJ*, **770**, 108
 Childress M. J., Wolf C., Zahid H. J., 2014, *MNRAS*, **445**, 1898
 Cohen M., Wheaton W. A., Megeath S. T., 2003, *AJ*, **126**, 1090
 Dhawan S., Jha S. W., Leibundgut B., 2018, *A&A*, **609**, A72
 Fakhouri H. K., et al., 2015, *ApJ*, **815**, 58
 Fitzpatrick E. L., 1999, *PASP*, **111**, 63
 Foley R. J., 2013, *MNRAS*, **435**, 273
 Foley R. J., Kirshner R. P., 2013, *ApJ*, **769**, L1
 Foley R. J., et al., 2012a, *AJ*, **143**, 113
 Foley R. J., et al., 2012b, *ApJ*, **753**, L5
 Foley R. J., et al., 2014, *MNRAS*, **443**, 2887
 Foley R. J., et al., 2016, *MNRAS*, **461**, 1308
 Friedman A. S., et al., 2015, *ApJS*, **220**, 9
 Graham M. L., et al., 2015, *MNRAS*, **446**, 2073
 Guy J., et al., 2007, *A&A*, **466**, 11
 Hicken M., Wood-Vasey W. M., Blondin S., Challis P., Jha S., Kelly P. L., Rest A., Kirshner R. P., 2009, *ApJ*, **700**, 1097
 Hoffmann S. L., et al., 2016, *ApJ*, **830**, 10
 Höflich P., Wheeler J. C., Thielemann F.-K., 1998, *ApJ*, **495**, 617
 Hsiao E. Y., et al., 2013, *ApJ*, **766**, 72

- Jeffery D. J., 1999, ArXiv Astrophysics e-prints,
 Jones D. O., et al., 2018, *ApJ*, **857**, 51
 Kelly P. L., Hicken M., Burke D. L., Mandel K. S., Kirshner R. P.,
 2010, *ApJ*, **715**, 743
 Kirshner R. P., et al., 1993, *ApJ*, **415**, 589
 Krist J. E., Hook R. N., Stoehr F., 2011, in Society of Photo-
 Optical Instrumentation Engineers (SPIE) Conference Series.
 , doi:10.1117/12.892762
 Lampeitl H., et al., 2010, *ApJ*, **722**, 566
 Lentz E. J., Baron E., Branch D., Hauschildt P. H., Nugent P. E.,
 2000, *ApJ*, **530**, 966
 Macri L. M., Stanek K. Z., Bersier D., Greenhill L. J., Reid M. J.,
 2006, *ApJ*, **652**, 1133
 Madore B. F., 1982, *ApJ*, **253**, 575
 Maguire K., et al., 2012, *MNRAS*, **426**, 2359
 Matheson T., et al., 2012, *ApJ*, **754**, 19
 Mazzali P. A., Podsiadlowski P., 2006, *MNRAS*, **369**, L19
 Mazzali P. A., et al., 2014, *MNRAS*, **439**, 1959
 Milne P. A., Brown P. J., Roming P. W. A., Bufano F., Gehrels
 N., 2013, *ApJ*, **779**, 23
 Milne P. A., Foley R. J., Brown P. J., Narayan G., 2015, *ApJ*,
803, 20
 Pan Y.-C., et al., 2015, *MNRAS*, **452**, 4307
 Pan Y.-C., Foley R. J., Filippenko A. V., Kuin N. P. M., 2018,
MNRAS,
 Pereira R., et al., 2013, *A&A*, **554**, A27
 Perlmutter S., et al., 1999, *ApJ*, **517**, 565
 Phillips M. M., 1993, *ApJ*, **413**, L105
 Phillips M. M., Lira P., Suntzeff N. B., Schommer R. A., Hamuy
 M., Maza J., 1999, *AJ*, **118**, 1766
 Podsiadlowski P., Mazzali P. A., Lesaffre P., Wolf C., Forster F.,
 2006, preprint, ([arXiv:astro-ph/0608324](https://arxiv.org/abs/astro-ph/0608324))
 Richmond M. W., Smith H. A., 2012, Journal of the American
 Association of Variable Star Observers (JAAVSO), **40**, 872
 Riess A. G., Press W. H., Kirshner R. P., 1996, *ApJ*, **473**, 88
 Riess A. G., et al., 1998, *AJ*, **116**, 1009
 Riess A. G., et al., 2009, *ApJS*, **183**, 109
 Riess A. G., et al., 2011, *ApJ*, **730**, 119
 Riess A. G., et al., 2016, *ApJ*, **826**, 56
 Sauer D. N., et al., 2008, *MNRAS*, **391**, 1605
 Scalzo R. A., et al., 2010, *ApJ*, **713**, 1073
 Schlafly E. F., Finkbeiner D. P., 2011, *ApJ*, **737**, 103
 Scolnic D. M., et al., 2018, *ApJ*, **859**, 101
 Shappee B. J., Stanek K. Z., 2011, *ApJ*, **733**, 124
 Silverman J. M., Ganeshalingam M., Filippenko A. V., 2013, *MN-
 RAS*, **430**, 1030
 Stetson P. B., 1987, *PASP*, **99**, 191
 Stetson P. B., 1994, *PASP*, **106**, 250
 Stetson P. B., 1996, *PASP*, **108**, 851
 Stritzinger M., et al., 2002, *AJ*, **124**, 2100
 Stritzinger M., Mazzali P. A., Sollerman J., Benetti S., 2006,
A&A, **460**, 793
 Stritzinger M. D., et al., 2011, *AJ*, **142**, 156
 Sullivan M., et al., 2010, *MNRAS*, **406**, 782
 Timmes F. X., Brown E. F., Truran J. W., 2003, *ApJ*, **590**, L83
 Tripp R., 1998, *A&A*, **331**, 815
 Tully R. B., Rizzi L., Shaya E. J., Courtois H. M., Makarov D. I.,
 Jacobs B. A., 2009, *AJ*, **138**, 323
 Walker E. S., Hachinger S., Mazzali P. A., Ellis R. S., Sullivan
 M., Gal Yam A., Howell D. A., 2012, *MNRAS*, **427**, 103
 Weyant A., et al., 2018, *AJ*, **155**, 201
 Yoachim P., McCommas L. P., Dalcanton J. J., Williams B. F.,
 2009, *AJ*, **137**, 4697
 Zhang K., et al., 2016, *ApJ*, **820**, 67